ULTRACOLD NEUTRON DETECTOR

A.G. Krivshich, V.A. Andreev, A.V. Vasiljev, E.A. Ivanov, D.S. Ilyin, A.P. Serebrov

1. Introduction

The problem of the neutron lifetime refinement is related with such important issues of particle physics and cosmology as verification of the Standard Model and the model of nucleosynthesis in the early stages of formation of our universe. By present, the highest accuracy of the neutron lifetime measurements has been achieved by the PNPI group [1, 2]: $t_n = 878.5 \pm 0.8$ s.

The aim of a new experiment is to still further improve the measurement accuracy to the level of 0.2 s. A new spectrometer has been developed to achieve this goal. It is based on the method of ultracold neutron (UCN) storage in a large gravitational trap (UCN source – PF2/MAM) at the Institute Laue–Langevin (ILL, Grenoble, France) [1].

The main spectrometer components were optimized: the volume of the trap was increased by more than a factor of 5, neutron losses on the walls of the trap were reduced due to a new hydrogen-free coatings, the working temperature was lowered down to 80–100 K, and the vacuum was improved to the level of 10^{-7} mbar.

An important part of the spectrometer is the UCN detector which was designed by the Track Detector Department HEPD (PNPI) in collaboration with the Neutron Physics Laboratory of the Neutron Research Division (PNPI).

2. Detector system

The UCN detector is the key unit of the spectrometer, whose working stability determines the accuracy of neutron counting during experimental runs and consequently determines also the accuracy of the neutron lifetime measurement. On this basis, the detector should meet the following requirements:

1. A high UCN detection efficiency, which requires a correct choice of the composition of the working gas mixture in order to reduce primary ionization charge losses in the detector gas volume in the vicinity of the cathode, as well as minimization of neutron losses in the entrance window.
2. Low noise level and low sensitivity to the background.
3. Reliability and long-term neutron counting stability, which is achieved by reduction of the gas leakage and by long-term maintenance of the working gas purity through proper selection of the materials used for the detector construction.

2.1. Detector construction

The design of the gas-filled detector is based on six independent proportional counters (cells), which are placed in a single gas volume. This guarantees that the gas mixture properties are identical in each proportional counter. This constructional concept has already proven itself well in previous experiments.

All counters have the cross-section of 48×46 mm^2 (height × width), the Au–W anode wire diameter is 25 μm. The lengths of the counters are optimized to cover the maximum detection area (Fig. 1). The respective counter lengths are 165 mm (1 and 6), 252 mm (2 and 5), and 287 mm (3 and 4). These counters are combined in two independent counting channels according to the scheme: 1, 3, 5 and 2, 4, 6.

The entrance window of 290 mm in diameter is made of a thin 100 μm aluminum foil in order to minimize UCN losses. The force acting on the foil at the working conditions is about 6.5 kN. Therefore, a special stainless steel grid is placed in front of the foil to support it from the neutron guide side (vacuum). The optimal pressure of the gas mixture is 1 bar (abs.).

Fig. 1. UCN detector parts: 1 – the upper part of the detector with the entrance window (the grid supporting the entrance foil is seen); 2 – the bottom part of the detector with six proportional counters; 3 – assembled UCN detector, shown from its back side (two preamplifiers and a gas manometer are seen)

2.2. Optimization of the electric field structure

The structure of the electric field within each of the proportional counters was optimized in order to minimize a negative impact of the detector design on the measured amplitude spectra.

1. Compared to the previous prototype, the design of the detector was changed to remove the drift space with non-uniform electric field that is located near the entrance window (Fig. 2).

2. The construction of the cathodes was optimized to provide a symmetrical structure of the electric field in the transverse direction of each anode wire.

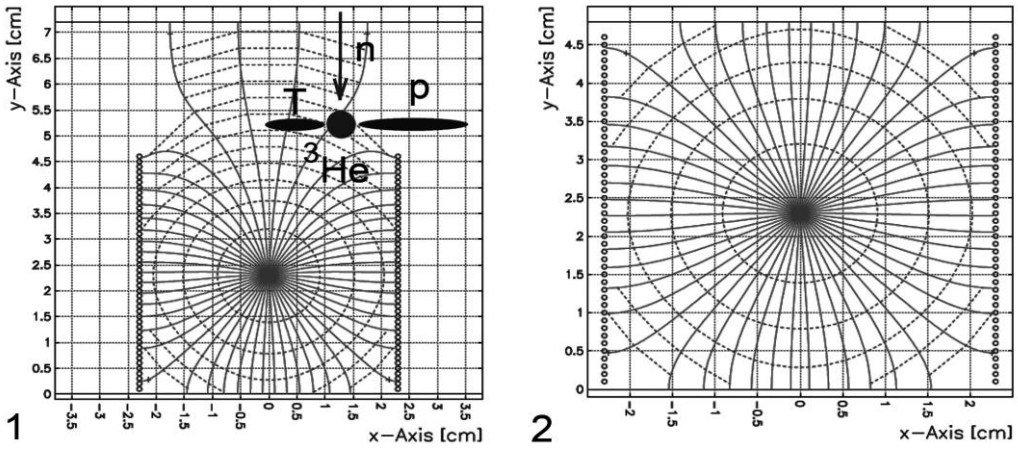

Fig. 2. The structure of the electric field and the timing diagrams in a cell calculated with GARFIELD [3] for a gas mixture 30 mbar ^{3}He + 970 mbar CF_4 and an anode voltage of 2 kV: 1 – prototype cell; 2 – improved cell. The *solid lines* are the drift lines of electrons; the *dotted lines* are the electron time contours in time steps of 0.1 μs

The measures taken greatly improved the detector characteristics:

1) a high uniformity of the gas gain along the anode wires was achieved and the maximal fluctuations did not exceed ±4%;

2) cross-talks between neighboring cells (counters) caused by ingress of parts of the proton–tritium tracks that trigger two independent events with smaller amplitudes were practically excluded (Fig. 2);

3) the maximum time required to collect the ions formed in a gas avalanche was reduced by more than a factor 8, thus not exceeding 10^4 μs.

2.3. Principle of ultracold neutron registration

The neutrons are detected through the nuclear reaction $^3\mathrm{He} + n \rightarrow p + T + 764$ keV. Since the reaction cross-section is inversely proportional to the neutron velocity v, one obtains $\sigma_{UCN} = \sigma(1.8\ \text{Å})\, v(1.8\ \text{Å})/v_{UCN}$, where $\sigma(1.8\ \text{Å}) = 5\,333$ b; $v(1.8\ \text{Å}) = 2\,200$ m/s; $v_{UCN} = 8$ m/s; $\sigma_{UCN} \approx 1.5 \cdot 10^6$ b.

In accordance with the momentum conservation law, the particles acquire kinetic energies $E(p) = 573$ keV and $E(T) = 191$ keV, respectively. They are emitted in opposite directions from the point of interaction and produce primary ionization charges. The centre of gravity (c. g.) of this charge cloud is shifted relative to the interaction point by a distance $R_{sph} = 0.35R(p)$, where $R(p)$ is the proton range. So, the c. g. of charges are placed on a spheroid surface of radius R_{sph} for all neutrons absorbed at the same point.

2.4. Detector efficiency and the "wall" effect

The key factor in achieving an effective rejection of the background from the "neutron" events is to minimize the "wall" effect [4], which is associated with a partial loss of the primary ionization charge near the cathode walls. The largest contribution comes from the tracks which are formed near the entrance window (Fig. 3).

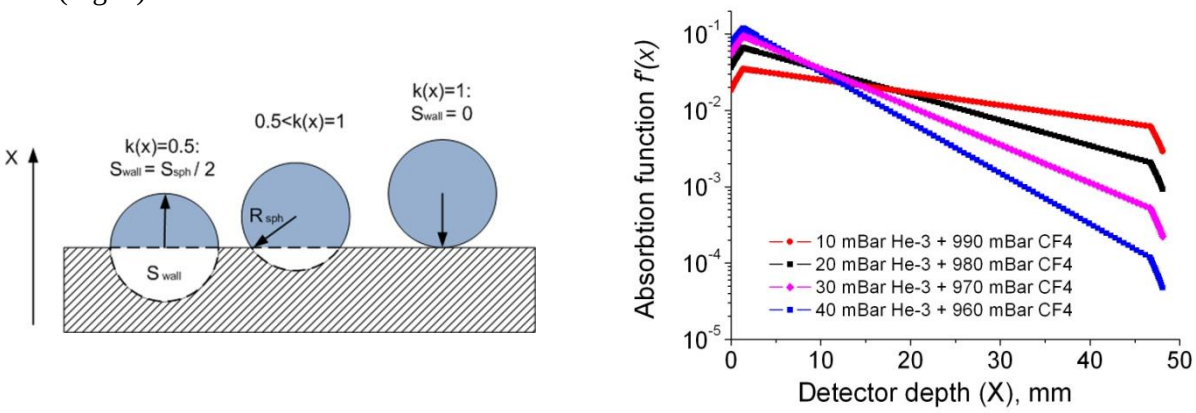

Fig. 3. The influence of the "wall" effect: the illustration for explaining the calculation of the correction factor $k(x)$ (*left*); the function $f'(x)$ for various compositions of the gas mixture (*right*)

The degree of influence of the "wall" effect is determined by two main factors: 1) the probability function $f(x)$ of the UCN absorption which depends on the partial pressure of ^{3}He; 2) the ranges of protons and tritons in the gas mixture, which are determined by the partial pressure of the stop-gas CF_4 or Ar.

The ranges of the particles were calculated with the SRIM program [5]. The results for Ar and CF_4 are $R_{sph}(CF_4) \approx 1.5/P$ [mm/bar] and $R_{sph}(\mathrm{Ar}) \approx 3.8/P$ [mm/bar], where P is the absolute gas pressure in bar.

The UCN absorption efficiency $\varepsilon(L)$ and the probability function of absorption $f'(x)$ are:

$$\varepsilon(L) = \int_0^L f'(x)dx,$$

$$f'(x) = f(x)k(x),\ \ f(x) = n\sigma e^{-n\sigma x},\ k(x) = 1 - S_{wall}/S_{sph},$$

where $L = 48$ mm is the detector thickness; n is the concentration of ^{3}He; σ is the cross-section for the reaction $^3\mathrm{He}(n, p)T$, and $k(x)$ is a correction factor accounting for the "wall" effect (front and back walls of the cell in the x direction). S_{wall} is the area of the circle segment with $r = R_{sph}$ truncated by the cathode wall, S_{sph} is the area of the full circle, and x is the coordinate along the beam direction (from the window to the back), as indicated in Fig. 3.

The correction factor $k(x)$ varies from 0.5 to 1. So, there are a few cases: 1) $k = 1$ for complete p–T tracks, 2) $0.5 < k < 1$ for truncated tracks, 3) $k = 0.5$ when the absorption point of the neutron (the centre of the spheroid) coincides with the wall surface. Events with $k < 0.5$ are not taken into account.

The "wall" effect value W of the cell takes into account all walls: $W = (1 - S/S_0)$, where

$$S_0 = \int_{X_{\min}}^{X_{\max}} \int_{Y_{\min}}^{Y_{\max}} f(x)dxdy$$

is the "effective" area of the cell ($X_{\min} = Y_{\min} = 0$ mm, $X_{\max} = 48$ mm, $Y_{\max} = 46$ mm) and

$$S_0 = \int_{X_{\min}}^{X_{\max}} \int_{Y_{\min}}^{Y_{\max}} f'(x)k(x)dxdy$$

is the "effective" area of the cell including wall effect corrections (front, back, and side walls of the cell), and $k(y)$ is the correction factor in the direction perpendicular to the x-axis and accounts for the side walls of the cell. The results of the calculations are shown in Fig. 4.

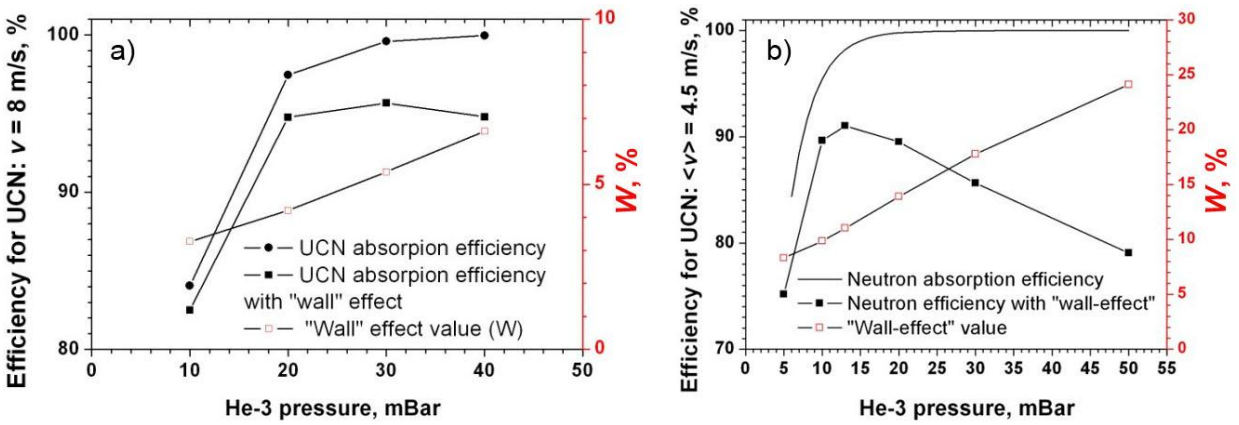

Fig. 4. Calculated efficiency and the "wall" effect value W versus the partial pressure of ^{3}He in the gas mixture: a – for the UCN velocity v = 8 m/s and the gas mixture ^{3}He–CF_4; b – for the average UCN velocity v = 4.5 m/s in the UCN spectrometer at the ILL and the gas mixture ^{3}He–Ar–CO_2. W is the fraction of truncated tracks in %

2.5. Choice of the gas mixture

The gas mixtures were carefully selected to minimize the "wall" effect and to achieve the maximal UCN efficiency.

For the initially planned UCN velocity v = 8 m/s, we choose the gas mixture ^{3}He–CF_4 which is conventional for thermal neutron detectors. For this gas mixture, the optimal pressure of ^{3}He is 30 mbar (see Fig. 4a). The maximal efficiency $\varepsilon_{UCN} \approx 95\%$ and a small "wall" effect value $W \approx 5.5\%$ were achieved for that ^{3}He pressure. The partial pressure of CF_4 was 1 030 mbar, limited by the maximum operational pressure (see Section 3.1).

The final composition of the gas mixture was optimized during detector tests under real experimental conditions. The real mean UCN velocity was $\langle v \rangle = 4.5 \pm 1.0$ m/s. For this case, the initial choice of the ^{3}He pressure 30 mbar was not optimal (see Fig. 4b), since the "wall" effect value $W \approx 17\%$ was high and the UCN efficiency $\varepsilon_{UCN} \approx 85\%$ was relatively low.

Therefore, the ^{3}He pressure was reduced to 13 mbar to achieve the maximal efficiency $\varepsilon_{UCN} \approx 91\%$ and to minimize the value of W down to $W \approx 11\%$. To reduce the operating voltage and consequently the high-voltage noise, the finally selected working gas mixture was 13 mbar ^{3}He + 1 060 mbar Ar + 20 mbar CO_2.

3. Detector tests

3.1. Lab tests (PNPI, Russia)

The detector was successfully tested both at the PNPI lab with a Pu–Be source and as a part of the UCN spectrometer at the PF2/MAM beam port of the ILL high-flux reactor in Grenoble. In particular, the gas gain non-uniformity along the anode wire was confined to be ±4 % for all cells, and the amplitude spectra were the same for both channels. An amplitude resolution $\Delta E/E$ = 6–15% (full width at half maximum) was obtained in the operating range of the anode high voltage HV = 1.7–1.9 kV.

3.2. Reactor tests (ILL, France)

The detector was installed at the UCN spectrometer at the HFR reactor in Grenoble. As mentioned before, the mean UCN velocity at the PF2/MAM beam port was $v = 4.5 \pm 1.0$ m/s. The initial measurements with a $^3He–CF_4$ gas mixture showed a significant number of "neutron" events with incomplete ionization tracks – low-amplitude tails in the amplitude spectra (Fig. 5a).

The impact of low-amplitude events on the amplitude spectra was significantly reduced by optimization of the gas mixture composition, as can be clearly seen in Fig. 5b from the counting rate reduction at the tritium energy level.

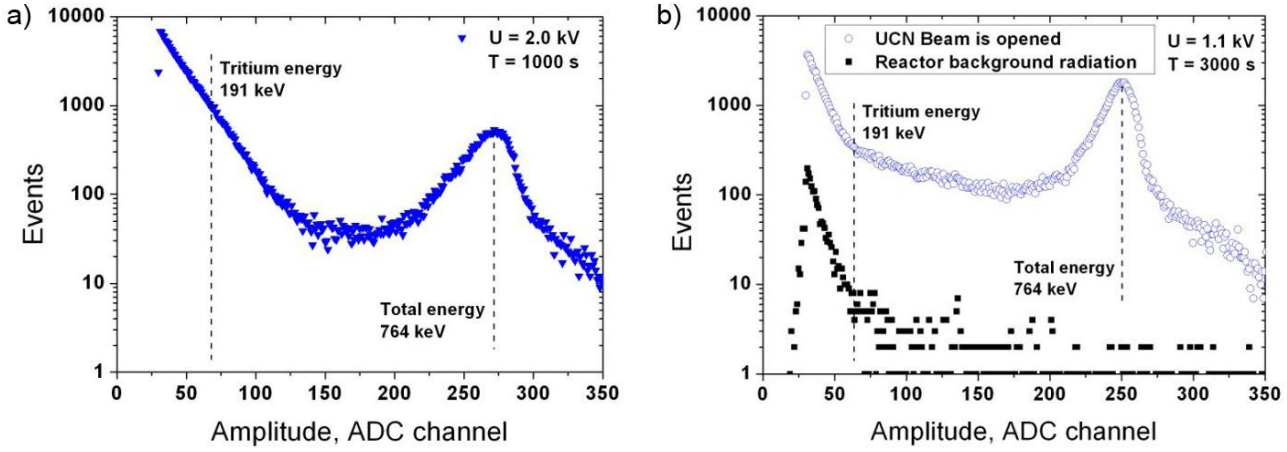

Fig. 5. Amplitude spectra obtained with the second counting channel of the detector at the UCN spectrometer at the HFR reactor with the thermal power 30 MW: a – for the $^3He–CF_4$ gas mixture (UCN irradiation); b – for the working gas mixture $^3He–Ar–CO_2$ (UCN and reactor background irradiation). Tritium and total reaction energy levels are indicated by *dotted lines*

Indeed, the gas mixture optimization improved the shape of the amplitude spectra, allowing for a more effective background rejection because a smaller number of "neutron" events were lost after amplitude discrimination.

4. Conclusion

The UCN detector has been designed and successfully tested. Currently it is used at the UCN spectrometer at the ILL Grenoble.

It has been shown that the influence of the "wall" effect on the structure of the UCN amplitude spectrum manifests itself in an additional continuous spectrum from background up to the total energy peak E_0 = 764 keV.

The negative impact of this effect offers a difficulty in rejecting background events from "neutron" events, since a significant number of such events have incomplete ionization tracks and, as a result, have low amplitudes.

This work was performed at the PNPI under a support of the Russian Science Foundation, the project No. 14-22-00105.

References

1. A. Serebrov *et al.*, J. Tech. Phys. **83**, No. 11, 136 (2013).
2. A. Serebrov *et al.*, Phys. Rev. C **78**, 035505 (2008).
3. R. Veenhof, Garfield – Simulation of Gaseous Detectors, http://consult.cern.ch/writeup/garfield
4. R. Batchelor *et al.*, Rev. Sci. Instrum. **26**, 1037 (1955).
5. J. Ziegler, Srim – the Stopping and Range of Ions in Matter, http://www.srim.org/